Determining the amplitude and timing of streamflow discontinuities: A cross wavelet analysis approach

Jan Adamowski[1]* and Andreas Prokoph[2,3]

[1] *Department of Bioresource Engineering, McGill University, 21 111 Lakeshore Road, Ste. Anne de Bellevue, QC, Canada, H9X 3V9*
[2] *Department of Earth Sciences, University of Ottawa, Marion Hall, Ottawa, ON, Canada, K1N 6N5*
[3] *Speedstat, Ottawa, ON, Canada, K1G 5J5*

Abstract:

Records of natural processes, such as gradual streamflow fluctuations, are commonly interrupted by long or short disruptions from natural non-linear responses to gradual changes, such as from river-ice break-ups, freezing as a result of annual solar cycles, or human causes, such as flow blocking by dams and other means, instrument calibrations and failure. The resulting abrupt or gradual shifts and missing data are considered to be discontinuities with respect to the normal signal. They differ from random noise as they do not follow any fixed distribution over time and, hence, cannot be eliminated by filtering. The multi-scale resolution features of continuous wavelet analysis and cross wavelet analysis were used in this study to determine the amplitude and timing of such streamflow discontinuities for specific wavebands. The cross wavelet based method was able to detect the strength and timing of abrupt shifts to new streamflow levels, gaps in data records longer than the waveband of interest and a sinusoidal discontinuity curve following an underlying modeled annual signal at ± 0.5 year uncertainty. Parameter testing of the time-frequency resolution demonstrated that high temporal resolution using narrow analysis windows is favorable to high-frequency resolution for detection of waveband-related discontinuities. Discontinuity analysis on observed daily streamflow records from Canadian rivers showed the following: (i) that there is at least one discontinuity/year related to the annual spring flood in each record studied, and (ii) neighboring streamflows have similar discontinuity patterns. In addition, the discontinuity density of the Canadian streamflows studied in this paper exhibit 11-year cycles that are inversely correlated with the solar intensity cycle. This suggests that more streamflow discontinuities, such as through fast freezing, snowmelt, or ice break-up, may occur during years with slightly lowered solar insolation. Copyright © 2013 John Wiley & Sons, Ltd.

KEY WORDS   streamflow discontinuity; continuous wavelet analysis; cross wavelet analysis; solar cycle; Canada

Received 24 July 2012; Accepted 25 March 2013

INTRODUCTION

Analysis of time series data is an important component in understanding hydrological systems. Discontinuities in normally persistent quasi-stationary streamflow signals, such as annual flow cycles, can provide insight into significant disruptions of the normal flow pattern. For example, gradual changes in forcing mechanisms, such as from the Earth's annual rotation around the sun can lead to non-linear responses such as abrupt freezing, ice break-up, snow melt, or flash floods from lake outbursts. These non-linear responses may not result in extreme flow magnitudes but in dilation or compression of the normal temporal flow pattern that form difficult to detect discontinuities. Other examples of discontinuities are those due to dam opening/closing, spill overflows,

saturation of wetlands or the closing of tributaries. The determination of such discontinuities can assist in understanding annual flow regimes, as well as contribute to identifying trends and forecasting events such as droughts. However, discontinuities in the long-term pattern can be hidden by higher frequency signals, such as noisy streamflow response to heavy rainfall and other short-term meteorological events or by missing or incorrect measurements.

Statistical methods of detecting abrupt changes in streamflow data include the segmented regression with constraints method and Pettitt's test (Pettitt, 1979). The segmented regression with constraints method allows for the detection of both shifts in trend and abrupt changes in hydrological data. Shao *et al.* (2010) applied the technique to analyse shift trends and change points in mean annual temperature, precipitation and runoff time series data in the Shiyang River Basin. Pettitt's test is a non-parametric statistical test that detects a significant change in the distribution of a time series, which may hint towards the existence of discontinuities. Although this

*Correspondence to: Jan Adamowski, Department of Bioresource Engineering, McGill University, 21 111 Lakeshore Road, Ste. Anne de Bellevue, QC, Canada, H9X 3V9
Email: jan.adamowski@mcgill.ca

method is able to detect such a change, it does not provide insight into the nature of the change (Zhao *et al*., 2011). A derivative of the Mann–Kendall test has been used to detect abrupt changes in climate records that can be also readily applied to streamflow records (Goossens and Berger, 1987). Fourier spectral analyses have also been used to study periodicities in streamflow time series data (Kunhel *et al*., 1990). However, Fourier analysis does not allow for the localization of a particular event in time and is not appropriate for non-stationary processes (Smith *et al*., 1998). These shortcomings are addressed by windowed short-term Fourier transform methods, such as the Gabor transform, although these methods do not allow for high resolution in both time and frequency.

The wavelet transform overcomes the problems of the methods described above and, thus, has been used as a time-series analysis method for detecting transient events in non-stationary processes in many applications. It transforms a time series into a frequency domain by simultaneously transforming the 'depth' or 'time' domain and the 'scale' or 'frequency' domain using various shapes and sizes of short filtering functions called wavelets. Jiang *et al*. (2002) introduced a method based on the Student's *t*-test to detect the coherency of abrupt changes between two time series, including one hydrological record. Their methods also provided significance estimates for the magnitude of the changes, and they also implemented a feature of the Haar wavelet transform for multi (frequency) separation of these changes. However, the method by Jiang *et al*. (2002) requires two time series; thus, it cannot distinguish the source (time series 1 or 2) of noise-related patterns.

The continuous wavelet transform (CWT) allows for the automatic localization of periodic signals, gradual shifts, abrupt interruptions, trends and onsets of trends in time series (Rioul and Vetterli, 1991; Mallat and Hwang, 1992). Similarly, the cross-wavelet transform allows for the automatic localization of periodic signals, gradual shifts, abrupt interruptions, trends and onsets of trends between two time series (e.g. Maraun and Kurths, 2004; Labat, 2010). As the wavelet function can be rescaled over a variety of timescales (Smith *et al*., 1998), abrupt changes or discontinuities in signal patterns can be located in terms of both time and frequency (Labat *et al*., 2000). Therefore, the onset time, duration and dominant frequencies of disturbances can be efficiently extracted with this technique. For example, an investigation of the capabilities of wavelet transforms for detecting signal disturbances in electrical power supply found the modulus maxima of wavelet transforms to be useful in isolating transient disturbances from the rest of the signal. However, in this study, only high-frequency disturbances were investigated, and so the efficiency of wavelet transforms for detecting lower-frequency or superimposed disturbances that are common in hydro-logical records (e.g. due to waveway blocking from dams or ice) was not determined (Nguyen and Hoang, 1999).

The multi-scale resolution feature of CWT allows for the detection and quantification of the amplitude and timing (phase) of low-frequency streamflow discontinuities of pre-determined wavelengths. The Morlet wavelet, which is a Gaussian modulated sine wave, has been used as the mother wavelet for detecting discontinuities in streamflow due to its good basic frequency resolution (Massei *et al*., 2011). Fraedrich *et al*. (1997) implemented a non-symmetric wavelet transform in a Mann-Kendall test and cluster-analysis based methodology to identify abrupt climate changes from flood levels of the Nile River.

Using XWT with the Morlet wavelet as the mother function has been shown to provide good time-frequency resolution suitable for water discharge or streamflow measurements (e.g. Labat, 2008, 2010). The stabilizing sinusoidal signal is incorporated by applying cross-wavelet analysis (XWT). Other types of wavelet transforms, such as the Mexican Hat and Haar wavelets, have also shown good local support (i.e. high accuracy in determination of temporal occurrences of cycles) in water discharge analysis (e.g. Smith *et al*. 1998) and may be applicable for discontinuity analysis.

This study focused on developing a methodology for detecting discontinuities in streamflow data using CWT and XWT, and tested the proposed method on a model data set and then applied it to streamflow data from Canadian rivers to identify patterns in streamflow discontinuities. In our proposed approach, we expand the approach of discontinuity detection of Jiang *et al*. (2002) to single hydrological or climate records by using, instead of a second record, an undisturbed stationary sinusoidal signal of the wavelength in which discontinuities are of interest. It should be noted that the Jiang *et al*. (2002) method is applied over all time scales to quantify the amplitudes and their significance. Our study is focused on specific time scales of interest and the counting of discontinuities that are above a specified threshold. Such temporal occurrences cannot be captured by student or other population, or autocorrelation-based tests. As such, our method does not include significance estimates comparable to those that were applied by Jiang *et al*. (2002).

METHODOLOGY

The proposed method consists of the following four main steps:

1. Time series of waveband specific discontinuity magnitudes are extracted using the XWT of individual meteorological or streamflow records coupled with a sine wave. The wavelength of the sine wave is set to

the frequency of interest (e.g. 365 days, 1 day etc.), which is determined by the goals set for individual investigation, for example, the 'impact of annual temperature variability on daily streamflow'.

2. Thresholds for discontinuity magnitudes are set from known abrupt record features such as artificial discontinuities arising from records gaps, or in the case of no gaps, above the mean discontinuity magnitude; above that, discontinuities are considered true and not noise related.

3. The number of discontinuities that are above the threshold are counted over a sliding time window and divided by the maximum number of possible discontinuities. This value is called the 'discontinuity density'. This results in discontinuity density records in the rational number scale that can be evaluated with data analysis methods designed for continuous records.

4. Fourier analysis is used to determine periodic patterns and their significance in the discontinuity record, and these are then compared with the spectral power of periodicities in the underlying hydrological records.

The proposed XWT-based methodology was tested on the following: (i) a model data set that combines complex signals (described later in the paper); and (ii) six streamflow records. The testing included fine tuning of wavelet transform specific parameters and comparison to discontinuity detection limits of the CWT. For testing purposes, the methodology was compared with a CWT-only discontinuity extraction method proposed by Labat et al. (2000).

The proposed method can be used for a wide variety of discontinuities. Some examples include the following: records of natural processes, such as gradual streamflow fluctuations, are commonly interrupted by long or short disruptions from natural non-linear responses to gradual changes, for example, from river-ice break-ups, snow melt, flash floods from lake outbursts, freezing as a result of annual solar cycles or human causes such as dam opening/closing, spill overflows, saturation of wetlands closing of tributaries, or instrument calibrations and failure. The resulting abrupt or gradual shifts and missing data are considered to be discontinuities with respect to the normal signal.

DATA ANALYSIS BACKGROUND

The method developed in this study for the detection and extraction of discontinuities in daily streamflow data involved discontinuity extraction based on the XWT for selected wavebands, which was found to be superior to extraction of discontinuities based solely on the CWT.

Continuous wavelet analysis

The wavelet coefficients W of a time series x(s) are calculated by a simple equation

$$W_\psi(a,b) = \left(\frac{1}{\sqrt{a}}\right) \int x(s)\psi\left(\frac{s\text{-}b}{a}\right)ds \qquad (1)$$

Where ψ is the mother wavelet, a is the scale factor that determines the characteristic frequency or wavelength and b represents the shift of the wavelet over x(s) (Prokoph and Barthelmes, 1996). The bandwidth resolution for a wavelet transform varies with $\Delta a = \frac{\sqrt{2}}{4\pi al}$ and a location resolution $\Delta b = \frac{al}{\sqrt{2}}$. Because of Heisenberg's uncertainty principle $\Delta a \Delta b \geq 1/4\pi$, the resolution of Δb and Δa cannot be arbitrarily small (e.g. Prokoph and Barthelmes, 1996). Parameter l is used to modify the wavelet transform bandwidth resolution either in favour of time or in favour of frequency.

In this study, the Morlet wavelet was used as the mother function (Morlet et al., 1982), which is expressed in its shifted and scaled version as

$$\Psi_{a,b}^l(s) = \sqrt[4]{\pi}\sqrt{al}\,\mathrm{e}^{-\frac{i2\pi(s-b)}{a}}\mathrm{e}^{-\frac{1}{2}\left(\frac{s-b}{al}\right)^2} \qquad (2)$$

The Morlet wavelet is a sinusoid with wavelength/scale a modulated by a Gaussian function (Torrence and Compo, 1998; Adamowski et al., 2009). Edge effects of the wavelet coefficients occur at the beginning and end of the analysed time series and increase with increasing wavelength (scale) and parameter l. Thus, a 'cone of influence of edge effects' is formed (Torrence and Compo, 1998). Influences of greater than 10% based on the wavelet analysis parameters used are illustrated in scalograms that are two-dimensional graphic presentations of the matrix of the wavelet coefficients $W(a,b)$, in the scale (or wavelength) time domain. The scalogram is coded with a colour scale (orange highest, blue lowest $W(a,b)$) for better graphical interpretation (Figure 3).

The wavelet coefficients W are normalized using the L1 normalization ($1/a$), replacing the commonly used $1/\sqrt{a}$ for L2 or L^2 normalization (see Equation 1). This allows wavelet coefficients to be interpreted in terms of Fourier amplitudes (e.g. Prokoph and Barthelmes, 1996). In addition, the L2 normalization of the Morlet wavelet commonly leads to overvaluing wavelet coefficients in long wavelengths compared with shorter ones (Schaefli et al., 2007).

Two parameters of l were tested for their precision in detecting wavelength-based discontinuities. A parameter of $l=6$ provides sufficiently precise results in the resolution of time and scale and is commonly suggested for hydrological records (e.g. Schaefli et al., 2007;

Adamowski *et al.*, 2009), whereas $l = 2$ provides better time resolution but loses most of the frequency resolution (Rioul and Vetterli, 1991). In this study, the CWT was used to detect and extract the wavebands, magnitudes and phases of signals embedded in the hydrological records. Abrupt changes in these features indicate waveband-dependent discontinuities in single records; these were then compared with the results of discontinuities extracted using the XWT (see below).

Cross-wavelet analysis (XWT)

The cross-wavelet spectrum W_{xy} of two series $x(s)$ and $y(s)$ is defined by

$$W_{xy}(a, b) = W_x(a, b) W_y^*(a, b) \quad (3)$$

where $W_x(a,b)$ and $W_y(a,b)$ are the CWT of $x(s)$ and $y(s)$, respectively, and * denotes the complex conjugate (e.g. Jury *et al.*, 2002). The phase difference is defined by

$$\Delta\Phi(b) = \tan^{-1} \frac{\int_{a1}^{a2} \text{Im}\left(W_{xy}(a, b)\right) da}{\int_{a1}^{a2} \text{Re}\left(W_{xy}(a, b)\right) da} \quad (4)$$

Im and *Re* indicate the imaginary and real parts, respectively. The mother wavelet and parameters used in this study are the same as for the CWT description provided above. More details on the XWT technique used in this study can be found in Maraun and Kurths (2004) and Labat (2008). As for the CWT in this study, the XWT applies the L1 normalization. Consequently, W_{xy} represents the cross amplitude between a stationary sinusoidal record with the wavelength of interest for discontinuity extraction and the real or modeled records.

Discontinuity extraction

A function $f(s)$ has a discontinuity of degree k at s_0, $k = 0$, $1, \ldots,$ if the k-th order left and right derivatives at t_0 are different; that is, $f^k(s_0 +) \neq f^k(s_0 -)$, the difference being the size of the discontinuity (Lee 1989). Using the CWT (see Equation 1) according to this definition, a discontinuity record u for each b between the time intervals $b-1$ and $b+1$ in a single time series can be interpreted as

$$u(b) = \sqrt{\sum_{a=1}^{n} \left(\frac{W(a, b)}{\sum W(b)} - \frac{W(a, b-1)}{\sum W(b-1)}\right)^2} \quad (5)$$

where n is the total number of frequencies. For waveband-specific discontinuity detection, the range of $a = 1$ to N can

be narrowed to a waveband of interest. The software used in this study (developed by Prokoph and Barthelmes, 1996) allows one to define the waveband of interest.

Extending the equation for discontinuity definition from one to two time series and using notations for XWT (Equation 3), the discontinuities v between two time series x and y can be accordingly expressed as

$$v(b) = \sqrt{\sum_{a=1}^{n} \left(\frac{W_{xy}(a, b)}{\sum W_{xy}(b)} - \frac{W_{xy}(a, b-1)}{\sum W_{xy}(b-1)}\right)^2} \quad (6)$$

The waveband of interest can be set by the user in the same way as for the CWT (see above). This waveband-specific XWT permits one to extract discontinuity records that are unaffected by high-frequency ('white') noise or long-term trends ('red noise') (Figure 3).

Model data set

A model data set was developed with the purpose of evaluating the accuracy of the waveband restricted discontinuity detection in a controlled environment with well-defined noise and gradual and abrupt short-term and long-term changes that occur at different wavelengths. The model data set has the following features (Figure 2A):

1. A stationary cosine background signal of annual wavelength (i.e. 365.25 days), which reflects a common annual streamflow cycle in Canadian rivers (Environment Canada, 1999);
2. A random high-frequency (white) noise at five times the amplitude of the periodic background signal (the resulting 1/5 signal-to-noise ratio limits the opportunity to detect the periodic signal by visual inspection);

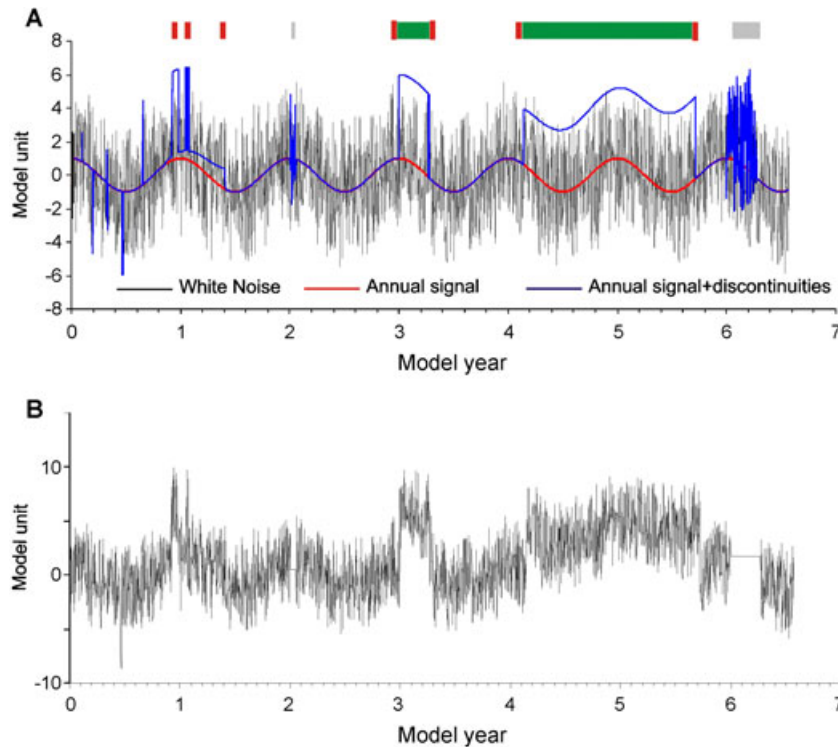Figure 1. Location of streamflow stations used with RHBN code (Table I)

Figure 2. Model data set of A, constituting four features (overlying 1-year cosine, white noise, spikes and level shifts), with the red bar indicating the onset and offset of discontinuities and the green bars showing the range of offset. B: Complete model including additions of gaps record (for details, see text)

3. Gaps in measurements of varying durations (see Figures 2B) (such gaps reflect missing/dismissed measurements mostly because of recording errors or suspension caused by administrative issues);
4. Short-term spikes and abrupt shifts > magnitude 1 of the mean values compared with the 100 days mean value; and
5. Abrupt shifts over 1 day and gradual shifts over 30 days or more with a subsequent return to normal conditions with magnitude 1, which simulates the influence of dams or changes in the drainage system.

The duration (~30–100 days) of the modeled shifts are based on the goal of finding patterns that are not confused with high-frequency noise of no long-term consequence or with long-term (multi-seasonal) shifts that will form gradual changes (trends) not subject to response to discontinuities but to long-term adaptation/changes. The magnitude of 1 in the presence of a noise magnitude of 5 was chosen to avoid detection of discontinuities by simple observation. The complete model data set, which incorporates the above described five features, is shown in Figure 2B.

The CWT of a simple cosine signal results in better wavelength (frequency) resolution using an analysis window size of $l=6$, whereas $l=2$ has smaller edge effects (Figures 3A and 3B), in accordance with the findings of previous research (e.g. Rioul and Vetterli,

1991). The testing of different wavelet analysis window sizes is essential to determine the optimal scale-to-time resolution because of Heisenberg's uncertainty (see above). The CWT of the more complex full model data set with the same choice of l illustrates that, despite the shortcomings in wavelength resolution, the use of $l=2$ enables better detection of discontinuities in the record (Figures 3C and D). In particular, the abrupt, large shift towards higher model values at 4.1 model years (Figures 2A and 3K) is well represented by an abrupt change in wavelet coefficients and wavelength with $l=2$ (Figures 3C) but not with $l=6$ (Figure 3D).

Many discontinuities are overprinted by white noise, particularly in short wavelengths. The XWT with the stationary annual cosine wave and the model enhances the discontinuities in the annual wand band for $l=2$ but smoothes out most discontinuities when $l=6$ is applied (Figures 3E, 3F and 3I). The XWT discontinuities extracted from the [0.5 year, 2 year] wavebands (Figures 3G and 3H) indicate that for $l=6$, only a single broad positive discontinuity anomaly occurs at the end of the model record covering the multi-year model-data gap (Figures 3J). In contrast, nine strong, well-localized (<0.5 years peak width) discontinuity anomalies are detectable using $l=2$ that can be mostly related to discontinuities of greater than 0.5-year duration (Figures 3J and 3K). The anomaly at each end of the model record is unrelated to the discontinuities and is
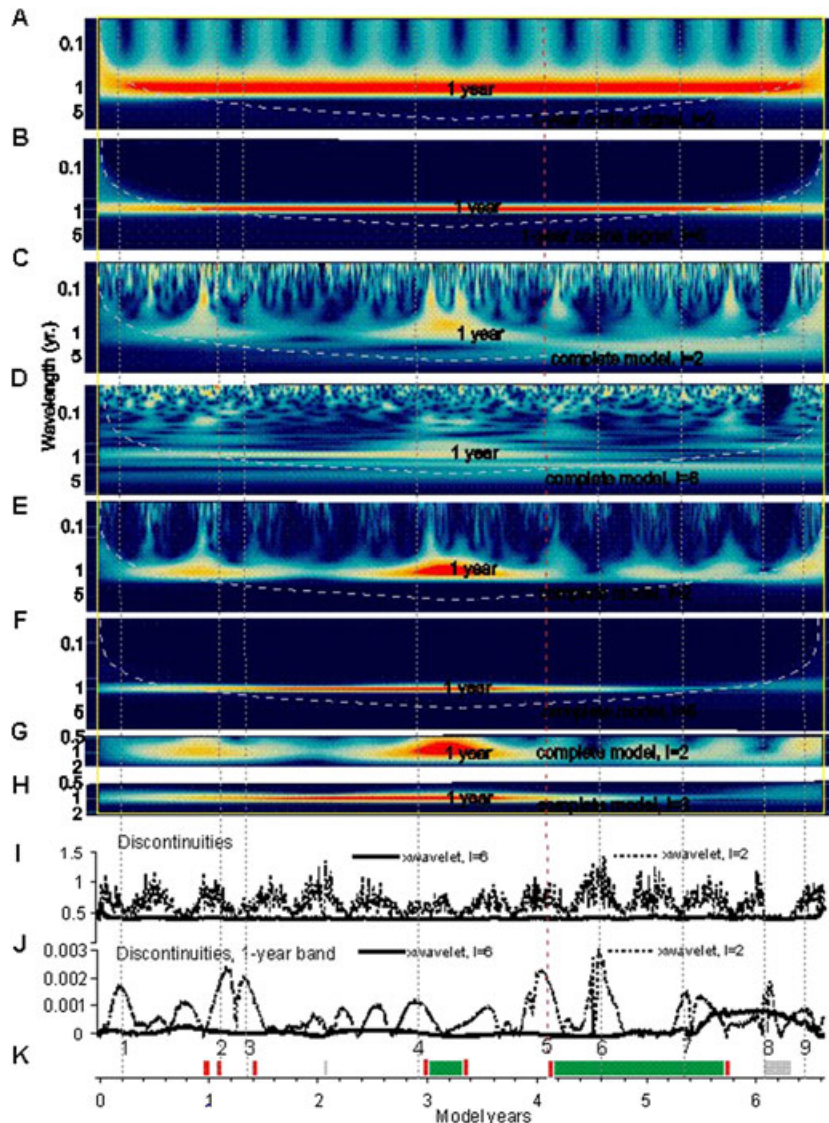
Figure 3. Steps of discontinuity detection from model data set (Figure 2B). Dashed lines show cone of influence (see text); vertical dashed lines delineate major discontinuities. Scalograms of A, CWT of cosine component using $l=2$; B, CWT of cosine component using $l=6$; C, CWT of complete model using $l=2$; D, CWT of complete model using $l=6$; E, XWT of complete model using $l=2$; F, XWT of complete model using $l=6$; G, XWT of complete model for [0.5,2] year wavebands using $l=2$; H, XWT of complete model for [0.5,2] year wavebands using $l=6$; I, XWT-discontinuities for entire waveband; and J, XWT-discontinuities for [0.5,2] year waveband

likely to be related to edge effects. Consequently, disconti-nuities can be best detected with a narrow analysis window and in record parts that are not influenced by edge effects.

STUDY SITES AND DATA

The proposed method was first tested on a simple cosine signal and then on the model data set to compare the precision of the different values of parameter l in detecting wavelength-based discontinuities. The method was then tested on Canadian daily streamflow records from different geographic locations. The hydrological data used in this study were extracted from the Reference Hydrometric Basin Network (RHBN) data sets produced by Environment Canada (1999), which include over a hundred records of annual maximum flows in Canadian rivers. The regularly extended sunspot number record (www.noaa.gov) was used for comparison with hydro-logical signals and discontinuities.

Six of the watersheds belonging to the RHBN were selected, from which daily streamflow data from a specific gauging station on each river were used (Table I and Figure 1). The watersheds were selected on the basis that they are pristine (i.e. unaltered by dams, canals or agricultural activity) and that data exist

Table I. Locations, ecological settings and record ranges of hydrological stations

ID RHCBN	ID EC*	Location	Drainage in km³	Region	Time range A.D.
85	01AD002	Saint John River at Fort Kent	14 700	Atlantic Maritime	1926–2009
165	08GA010	Capilano River above Intake	172	Pacific Maritime	1914–1955,1958–2009
29	05PB014	Turtle River near Mine Centre	4870	Boreal Shield	1920–1979,1984–2009
4	05AD005	Belly River near Mountain View	319	Montane Cord.	1912–2010
6	05BB001	Bow River at Banff	2210	Montane Cord.	1910–2010
X1	02KF006	Mississippi River at Appleton	2900	Mixedwood Plain	1918–2009

*EC Environment Canada

for over 40 years. It was also ensured that five of the southern Canadian ecozones were represented (Table I). The ecozones are defined based on vegetation, wildlife, latitude, altitude, proximity to oceans, terrain and other criteria (Environment Canada, 1999). However, the Mississippi River at Appleton (watershed X1) is not part of the RHBN but was included in the selection as it is the only long-term daily record representative of its ecozone.

Because the watersheds were chosen to represent five different ecozones, there is considerable variation between them in terms of climate and patterns of precipitation and streamflow. Eastern Ontario and southern Quebec (watersheds 85 and X1) have a continental climate with long, cold winters and short, humid summers (Zhang *et al.*, 2001; Adamowski *et al.*, 2012). The streamflow pattern in these regions is generally charac-
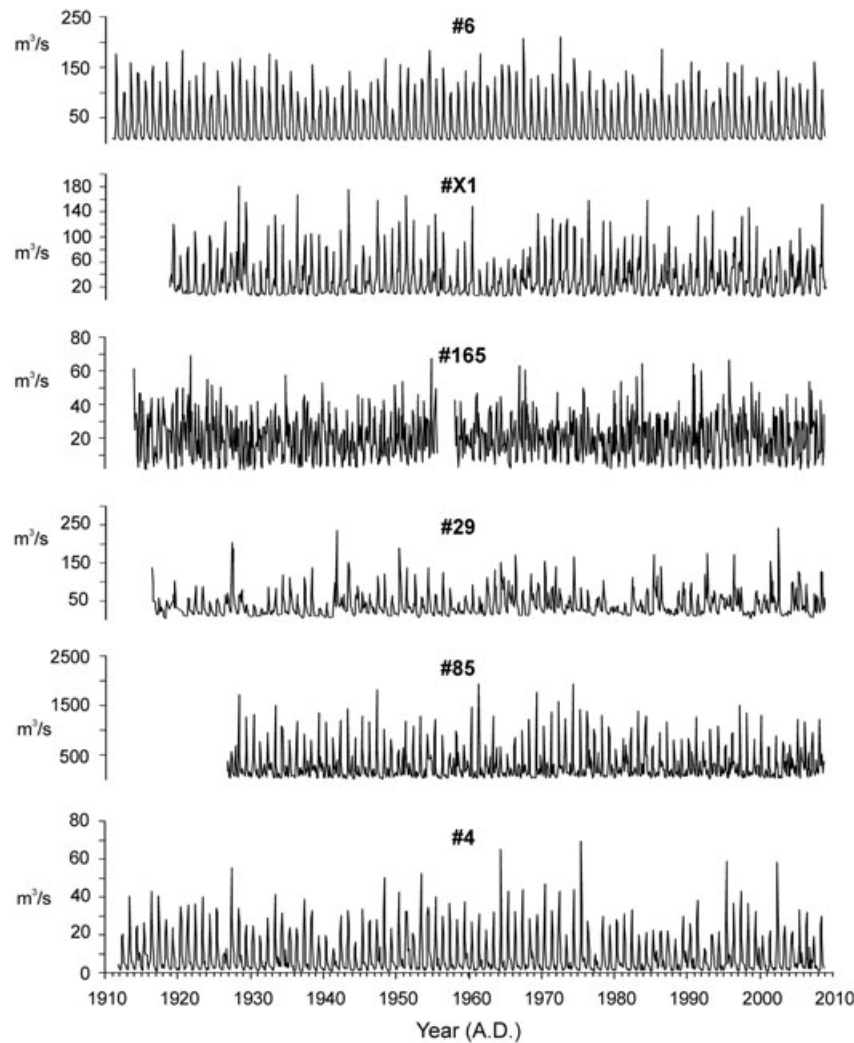

Figure 4. Canadian daily streamflow records. Station locations are shown in Table I and Figure 1

terized by a spring flood related to snowmelt and relatively low flows during the remainder of the year (Adamowski, 2008). The Canadian Shield area of northwestern Ontario (watershed 29) has a strongly continental climate, with large seasonal differences in temperature. The climate is relatively moist, with the summer months (i.e. between May and September) being the wettest. The majority of precipitation outside this period falls as snow (St George, 2007). By contrast, southern Alberta (watershed 4) experiences a cool, semi-arid climate, as it lies in the rain shadow of the Rocky Mountains (Byrne *et al.*, 1989). Watershed 6 at Banff, Alberta experiences a similar climate as it is located on the eastern side of the Rocky Mountains.

Finally, coastal British Columbia (watershed 165) has a more maritime climate with moderate temperatures and high precipitation that predominantly falls as rain rather than snow during the winter (Shaefer, 1978).

RESULTS AND DISCUSSION

Statistical tests based on the recommendations of Shiao and Condie (1980) were carried out to verify the quality of the RHBN data (Environment Canada, 1999). All of the records start before 1930 and last until at least 2009, with two of the records exhibiting several gaps (Figure 4,
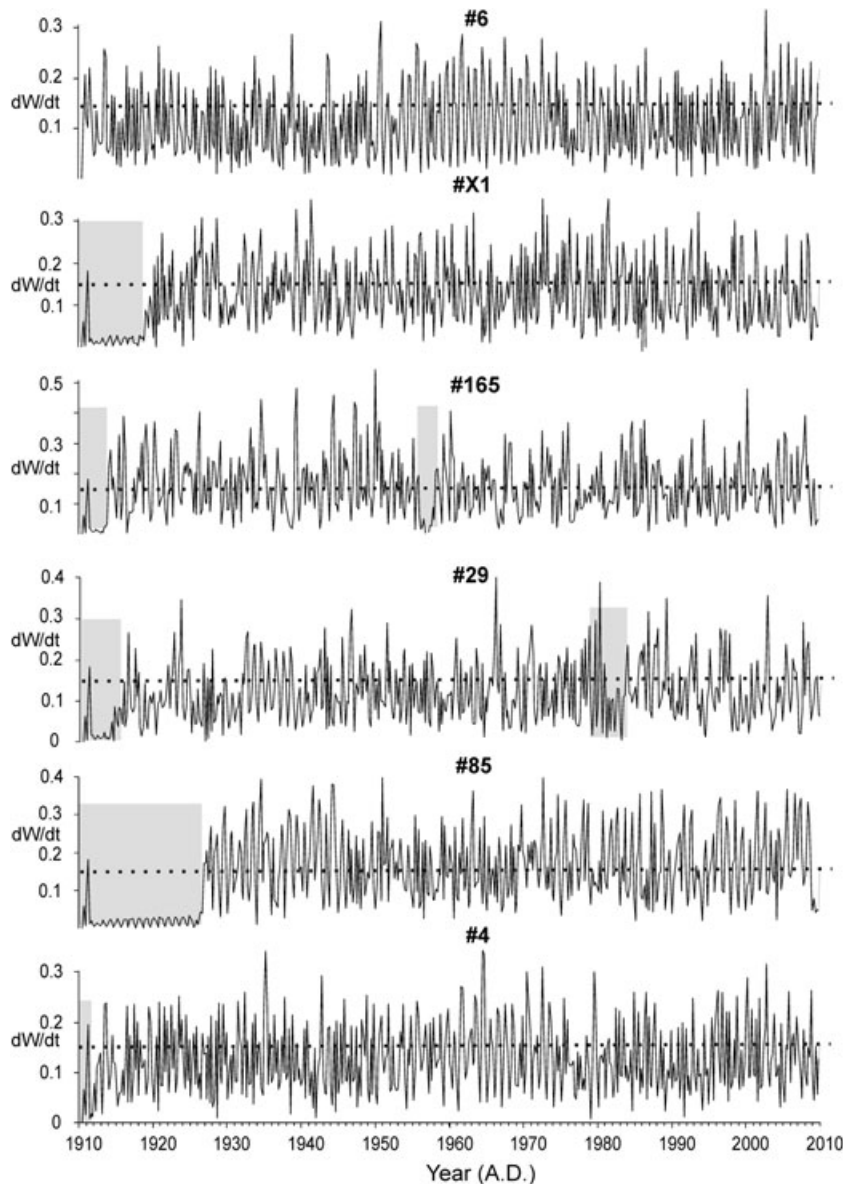

Figure 5. Discontinuities (g = dW/dt) of daily streamflow data in [0.5, 2] year waveband using $l = 2$. Gray shaded areas mark missing data in the records. Dashed line delineates discontinuity threshold of dW/dt = 0.15 that has been used for discontinuity density calculations

Table I). Records of sunspot data corresponding to the same time interval as the streamflow records were collected from the NOAA Web page.

At first, the annual waveband ([0.5, 2] year) was investigated for discontinuities because fluctuations on an annual scale exhibit the most important fluctuations in Canadian streamflows, such as spring flood due to snow melt and summer droughts (e.g. Zhang *et al.*, 2001). Discontinuity analysis for the [0.5, 2] year waveband shows that missing data at the beginning and in the middle of the records are easily identified by low discontinuity values (Figure 5). As expressed in the methodology, the discontinuity threshold is best obtained from *dW/dt* across data gaps. Based on this definition, a threshold discontinuity value of 0.15 in the annual waveband was derived for all records based on data gaps and mean discontinuity value. The mean discontinuity value ranges from 0.11 to 0.15 despite the different hydrological settings for the streamflows. The similar range of the discontinuity from 0 to ~3.5 *dW/dT* (Figure 5) also indicates that the same discontinuity threshold for all analysed record is reasonable. Only record times that have discontinuity values above 0.15 had a nominal discontinuity count assigned (yes = 1, no = 0).
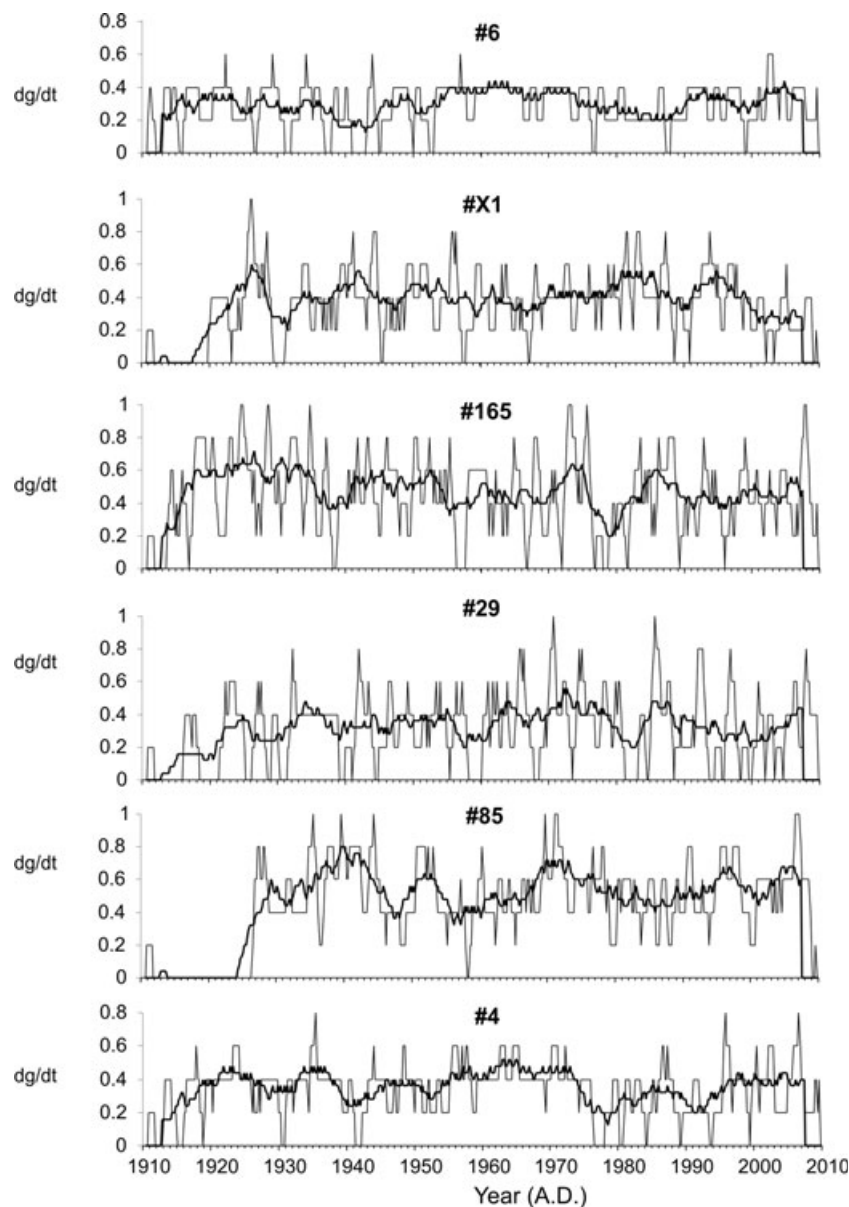

Figure 6. Discontinuity density (dg/dt) for all records averaged over 1 and 5 years. Note that the parts of sections that have data missing were excluded from averaging

A single large discontinuity was observed at the beginning of the record for five of the six watersheds, indicating an edge effect response (Figure 4J). Otherwise, no obvious pattern in discontinuity is discernible, apart from correspondence between watersheds 4 and 6, which are located within the same ecozone (Table I and Figure 1). These watersheds exhibited only one discontinuity above 0.15 per year in the 1960s (Figure 5).

The nominal discontinuity assignments above the threshold of 0.15 were calculated over 1- and 5-year windows, providing a maximum resolution for the 1-year waveband and a high-robustness estimate, respectively. The discontinuity densities were high in the late 1950s and 1970s, and low in the late 1970s in all records, and generally show a pronounced cyclical nature (Figure 6). The 5-year average of all discontinuity density records exhibits a pronounced 11-year periodicity. Cross-correlation with the sunspot number record shows that the discontinuity density in Canadian streamflows is approximately inversely correlated with the ~11-year periodic solar intensity variability (Figure 7). The total averaged streamflow from the selected Canadian stations generally also decreases when there are less discontinuities, although the decrease is less obvious (Figure 7). In addition, an 11-year cyclicity in total averaged streamflow is subdued by a stronger bi-decadal cyclicity (Figures 7 and 8). In this particular example, the results indicate that more discontinuities occur during years of decreased solar radiation and that there is a weak correlation between the densities of discontinuities and the streamflow in general. We argue that during lower solar intensity years, the seasonal climate regimes change more abruptly in mid-latitude settings in Canada. The subsequent more rapid onsets of freezing and ice break-up, as well as more
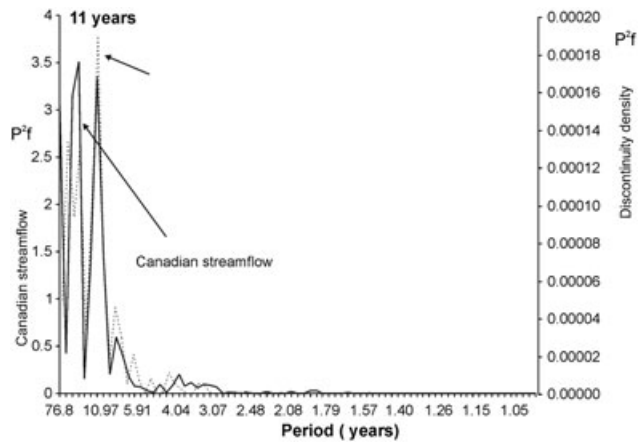

Figure 8. Spectral analysis of 5-year averaged streamflow record from the selected Canadian stations (blue) and discontinuity density records (red)

frequent short-term weather fluctuations, may lead to more abrupt changes in the streamflow pattern as shown with larger spring floods in the Rocky Mountains of Canada during low solar intensity years (Prokoph et al., 2012).

The proposed methodology of discontinuity detection and analysis could also be used to evaluate the effects of other natural (e.g. El Nino, monsoon, streamflow change because of landslides) or human-made (e.g. waterway widening and cleaning) phenomena on abrupt changes in streamflow patterns. Furthermore, the proposed method allows one to remove the influence of already known discontinuities (e.g. known streamflow magnitude jumps due to dam opening and closing). This allows one to focus on detection and interpretation of discontinuities occurring in the waveband of interest.
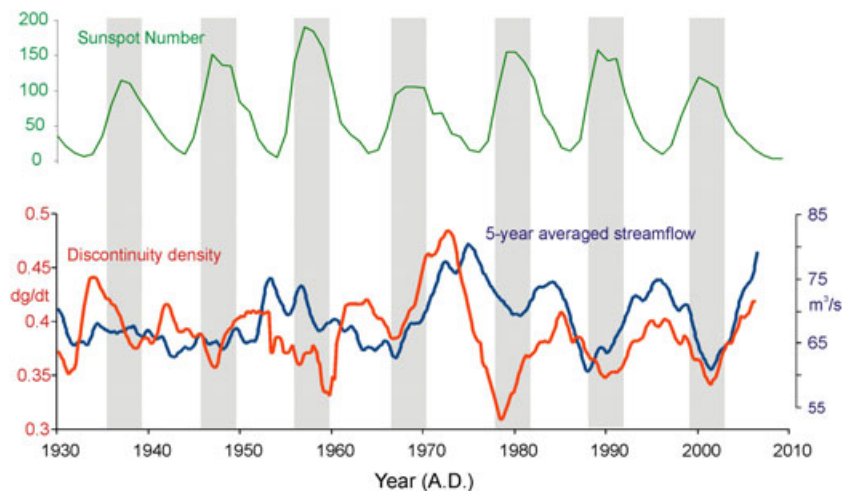

Figure 7. Annual sunspot numbers (source: www.noaa.gov), 5 years averaged discontinuity density of all streamflow records, and 5 years averaged streamflow record from the selected Canadian stations

CONCLUSION

The proposed methodology is designed to detect streamflow discontinuities that are significant for periods (wavelengths) of interest. Practical examples of such discontinuities would be those due to dam opening/closing, spill overflows, saturation of wetlands or closing of tributaries. It is shown that the XWT of the observed record as the first time series and a stationary sinusoidal signal of wavelength of interest can detect and extract such discontinuities specific for the wavelength of interest. In particular, discontinuities at the onset and offset of a shift in the mean of the records for at least half of the duration of the wavelength of interest can be detected and separated from other signals and noise. Parameter testing of the time-frequency resolution of the Morlet wavelet shows that high time resolution is favorable to high-frequency resolution for detection of waveband-related discontinuities.

The application of the proposed methodology on a model data set shows that the strength and timing of abrupt shifts to a new lower or higher streamflow level, gaps longer than the waveband of interest, and a sinusoidal discontinuity curve following an underlying modeled annual signal are detected at ±0.5 year uncertainty.

Discontinuity analysis on observed daily streamflow records shows the following: (i) that each record has at least one discontinuity/year related to the annual spring-flood, (ii) that neighboring streamflows have similar discontinuity patterns, and (iii) the discontinuity densities in Canadian rivers follow an 11-year cycle inverse to the solar intensity cycle. An 11-year cycle is also evident in the raw streamflow records but is less pronounced.

The proposed methodology was applied to streamflows in Canada but can be similarly used in other parts of the world. This could include the effects of the onset and end of the monsoon or changes in the onset of annual snowmelt over time. Other wavelet types such as the Haar wavelet may also be useful for this type of detection because of their excellent local support. This study focused primarily on discontinuities in the annual streamflow pattern but could be further used for studies to evaluate the effect of discontinuities on other time scales, for example, the influence of abrupt changes of oceanic-atmospheric oscillation patterns on forming abrupt streamflow pattern changes. The methodology that is proposed and presented in this paper is able to extract streamflow discontinuities in specified wavelength and defined thresholds. For future studies, a method of testing the significance of the thresholds would be beneficial.

REFERENCES

Adamowski J. 2008. Development of a short-term river flood forecasting model for snowmelt driven floods based on wavelet and cross-wavelet analysis. *Journal of Hydrology* **353**: 247–266.

Adamowski K, Prokoph A, Adamowski J. 2009. Development of a new method of wavelet aided trend detection and estimation. *Hydrological Processes* **23**: 2686–2696.

Adamowski JF, Prokoph A, Adamowski K. 2012. Spatial temporal changes in streamflow patterns in eastern Ontario and southwestern Quebec, Canada and their relation to precipitation changes. *International Journal of Climate Change: Impacts and Responses* **3**(1): 155–170.

Byrne JM, Barendregt R, Schaffer D. 1989. Assessing potential climate change impacts on water supply and demand in southern Alberta. *Canadian Water Resources Journal* **14**(4): 5–15.

Environment Canada. 1999. Establishment of the reference hydrometric basin network (RHBN) for Canada. *Environment Canada, Ottawa*: 42 p.

Fraedrich K, Jiang J, Gerstengarbe W. 1997. Multiscale detection of abrupt climate changes: Application to Nile River flood levels. *International Journal of Climatology* **17**: 1301–1315.

Goossens C, Berger A. 1987. How to recognize an abrupt climatic change?, In Abrupt Climatic Change, Berger WH, Labeyrie LD (eds). D Reidel Publisher: Dordrecht 31–45.

Jiang J, Mendelssohn R, Schwing F, Fraedrich K. 2002. Coherency detection of multiple abrupt changes in historic Nile flood levels. *Geophysical Research Letters* **29**: 1121–1124.

Jury MR, Enfield DB, Mélice J. 2002. Tropical monsoons around Africa: Stability of El Niño–Southern Oscillation associations and links with continental climate. *Journal of Geophysical Research* **107**: 3151–3167.

Kunhel I, McMahon TA, Finlayson BL. 1990. Climatic influences on streamflow variability: A comparison between southeastern Australia and southeastern United States of America. *Water Resources Research* **26**: 2483–2496.

Labat D. 2008. Wavelet analysis of the annual discharge records of the world's largest rivers. *Advances in Water Resources* **31**: 109–117.

Labat D. 2010. Cross wavelet analyses of annual continental freshwater discharge and selected climate indices. *Journal of Hydrology* **385**: 269–278.

Labat D, Ababou R, Mangin A. 2000. Rainfall-runoff relations for karstic springs. Part II: Continuous wavelet and discrete orthogonal multiresolution analyses. *Journal of Hydrology* **238**: 149–178.

Lee L, Huang L, Chao J. 1989. On the stability of rotational discontinuities and intermediate shocks. *Journal of Geophysical Research: Space Physics* **94**: 8813–8825.

Mallat S, Hwang WL. 1992. Singularity Detection and Processing with Wavelets. *IEEE Transactions on Information Theory* **38**: 617–639.

Maraun D, Kurths J. 2004. Cross wavelet analysis: significance testing and pitfalls. *Nonlinear Processes in Geophysics* **11**: 505–514.

Massei N, Laignel B, Rosero E. 2011. A wavelet approach to the short-term to pluri-decennial variability of streamflow in the Mississippi river basin from 1934 to 1998. *International Journal of Climatology* **31**: 31–43.

Morlet J, Arehs G, Fourgeau I. 1982. Wave propagation and sampling theory. *Geophysics* **47**: 203–236.

Nguyen DT, Hoang TA. 1999. Detection of disturbances on electricity supply using wavelets. *Australasian Universities Power Engineering Conference and IEAust Electric Energy Conference*: 184–189.

Pettitt AN. 1979. A nonparametric approach to the changepoint problem. *Applied Statistician* **28**: 126–35.

Prokoph A, Barthelmes F. 1996. Detection of nonstationarities in geological time series: Wavelet transform of chaotic and cyclic sequences. *Computer & Geosciences* **22**: 1097–1108.

Prokoph A, Adamowski J, Adamowski K. 2012. Influence of the 11 year solar cycle on annual streamflow maxima in Southern Canada. *Journal of Hydrology* **442–443**: 55–62.

Rioul O, Vetterli M. 1991. Wavelets and Signal Processing. *IEEE Signal Processing Magazine* **8**: 14–38.

Schaefli B, Maraun D, Holschneider M. 2007. What drives high flow events in the Swiss Alps? Recent developments in wavelet spectral analysis and their application to hydrology. *Advances in Water Resources* **30**: 2511–2525.

Shaefer DG. 1978. Climate. In The soil landscapes of British Columbia, B. C., Valentine KWG, Sprout PN, Baker TE, Lavkulich LM (eds). The

soil landscapes of British Columbia, B.C. Ministry of Environment, Resource Analysis Branch: Victoria; 197.

Shao Q, Li Z, Xu Z. 2010. Trend detection in hydrological time series by segment regression with application to Shiyang River Basin. *Stochastic Environmental Research and Risk Assessment* **24**: 221–233.

Shiao SY, Condie R. 1980. Statistical tests for independence, trend, homogeneity and randomness. Inland Waters Directorate, Environment Canada.

Smith LC, Turcotte DL, Isacks BL. 1998. Stream flow characterization and feature detection using a discrete wavelet transform. *Hydrological Processes* **12**: 233–249.

St George S. 2007. Streamflow in the Winnipeg River basin, Canada: Trends, extremes and climate linkages. *Journal of Hydrology* **332**: 396–411.

Torrence C, Compo GP. 1998. A practical guide to wavelet analysis. *Bulletin of the American Meteorological Society* **79**: 61–78.

Zhang X, Harvey K, Hogg WD, Yuzyk R. 2001. Trends in Canadian streamflow. *Water Resources Research* **37**: 987–998.

Zhao F, Xu Z, Zhang L. 2011. Changes in streamflow regime following vegetation changes from paired catchments. *Hydrological Processes* Doi:10.1002/hyp.8266